PIT SLOPE FAILURE EVALUATION IN NEAR REAL TIME USING UAV PHOTOGRAMMETRY AND 3D LIMIT EQUILIBRIUM ANALYSIS

Neil Bar[1], Michael Kostadinovski[1], Michael Tucker[1], Glen Byng[1], Rully Rachmatullah[1], Arturo Maldonado[1], Markus Pötsch[2], Andreas Gaich[2], Alison McQuillan[3] and Thamer Yacoub[3]

[1]BHP, Perth, Australia, [2]3GSM GmbH, Graz, Austria, [3]Rocscience Inc., Toronto, Canada

ABSTRACT

Slope failures are an inevitable aspect of economic pit slope designs in the mining industry. Large open pit guidelines and industry standards accept up to 30% of benches in open pits to collapse provided that they are controlled and that no personnel are at risk. Rigorous ground control measures including real time monitoring systems at TARP (trigger-action-response-plan) protocols are widely utilized to prevent personnel from being exposed to slope failure risks.

Technology and computing capability are rapidly evolving. Aerial photogrammetry techniques using UAV (unmanned aerial vehicles) enable geotechnical engineers and engineering geologists to work faster and more safely by removing themselves from potential line-of-fire near unstable slopes. Slope stability modelling software using limit equilibrium (LE) and finite element (FE) methods in three dimensions (3D) is also becoming more accessible, user-friendly and faster to operate. These key components enable geotechnical engineers to undertake site investigations, develop geotechnical models and assess slope stability faster and in more detail with less exposure to fall of ground hazards in the field.

This paper describes the rapid and robust process utilized at BHP for appraising a slope failure at an iron ore mine site in the Pilbara region of Western Australia using a combination of UAV photogrammetry and 3D slope stability models in less than a shift (i.e. less than 12 hours).

1 INTRODUCTION

In both civil engineering and mining projects, practical limitations significantly affect the ability to assess the stability of rock slope cuttings and benches in real-time, using analytical approaches such as kinematics, LE, FE or distinct element modelling. Excavation is usually *too fast* for this (Barton & Bar, 2015). Two key limitations currently preventing this are:

1. Time required for local site investigations. In the case where slope failures occur, safety concerns and residual risks in close proximity to unstable slopes such as failure reactivation or localized rock falls may prevent site investigations altogether, and
2. Time required to translate the site investigation data into a geotechnical model to facilitate detailed stability analysis using a variety of numerical codes.

Traditional rock slope mapping techniques would typically require from 30 to 180 minutes of field time to assess a 10 metre length of slope using window and traverse approaches, respectively. Development or refinement of a geotechnical model and subsequent stability analyses can easily take several hours thereafter. In contrast, empirical methods such as SMR (Pastor et al. 2019; Romana, 1985; Romana, 1995), Q-Slope (Barton & Bar, 2015; Bar & Barton, 2017; Bar & Barton, 2018) and SSAM (McQuillan, 2019; McQuillan et al. 2018) can be applied in real-time to assess stability as slopes are exposed in the field. Typically, these empirical methods require between 5 and 15 minutes in the field to assess slope stability for a 10 metre long section.

Slope stability modelling techniques have significantly improved over the years from basic kinematic analysis in the 1990s through to two-dimensional (2D) LE analysis and simple finite element modelling using PC's in the 2000s (Bar & Weekes, 2017). However, in Australian iron ore and coal deposits, open pit mines are typically designed using relatively limited data density and the routine use of more advanced numerical modelling techniques such as FLAC and UDEC is generally not practicable, nor is it always warranted. McQuillan et al. (2019) indicated that over 80% and 90% of coal mines are designed using kinematics and 2D LE analysis, respectively; and that less than 15% of designs include 3D numerical analyses. The recent development and improvement of simple-to-use 3D LE and FE analysis software has provided an additional method for identifying potential issues in slope designs (Bar & McQuillan, 2018; Bar et al. 2019). The use of 3D analysis has also been shown to provide more detailed analysis results that allow geotechnical engineers to optimize pit slope designs and unlock resource value (Bar et al. 2018).

2 WESTERN AUSTRALIA IRON ORE

The central and eastern Pilbara region of Western Australia is renowned for its abundance of economically extractable, bedded iron ore deposits between the townships of Newman and Port Hedland. BHP Limited currently operates over 50 individual open cut mines across six mining hubs: Whaleback, Eastern Ridge, Jimblebar, Yandi, Mining Area C and South Flank (Figure 1). Due to the broad regional expanse of the operations, a very high extraction rate is achieved despite vertical development rates remaining relatively low (typically one to three benches or 10 to 30 metres per year in an individual iron ore pit). Final pit depths generally range from less than 100 to 450 metres.

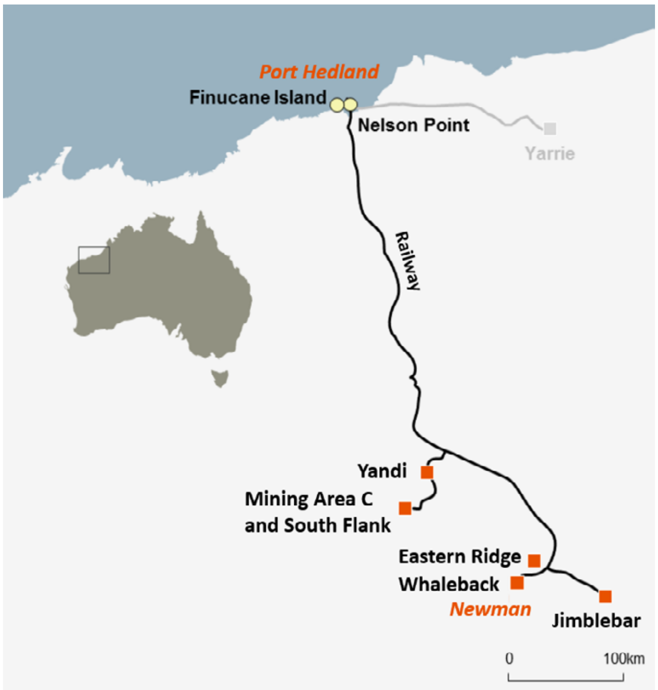

Figure 1: Location of BHP Limited Western Australia iron ore operations

Iron ore deposits in the Pilbara region occur within banded iron formations of the Hamersley Group which comprises Archaean to Proterozoic marine sedimentary and volcanic rocks (Perring & Hronsky, 2019). Geological structures play a key role in the location, geometry and preservation of high grade iron ore bodies. The structural evolution of the Hamersley province is considered to be well understood and is documented in Dalstra (2014). In general terms, it comprises normal faulting and thick-skinned tectonics in the west and more intense folding, minor thrust faulting and possible thin-skinned tectonics in the east. Some deposits, such as Whaleback, are very complex with several phases of deformation resulting in an overturned stratigraphic sequence. The stratigraphic units of economic interest consist of banded iron formation (BIF) with interbedded carbonates and shales. BIF can vary in thickness due to differing amounts of carbonate dissolution and silica replacement during iron ore enrichment formation (Harmsworth et al. 1990) and typically contain thick interbedded shale bands, some of which make excellent stratigraphic marker horizons in the mining areas as they are remarkably persistent across hundreds of kilometres throughout the Hamersley province.

The bedded iron ore deposits are hosted in highly anisotropic rock masses. Anisotropy, as defined in engineering geology, refers to a rock whose engineering properties (such as strength and permeability) vary with direction. Anisotropy is very common and present everywhere. Isotropy is rare (Barton & Quadros, 2015). Anisotropy is produced as a consequence of the geological history of the rock or rock mass, and generally has its origins in the varying mineralogical composition of different layers and/or a preferred orientation of mineral grains. Distinctive bedding planes are produced in sedimentary rocks due to depositional cycles as is the case in iron ore. Two distinct scales of anisotropy are prevalent (Figure 2):

1. Bedding scale – between individual bedding planes (e.g. BIF-BIF or shale-shale bedding planes).
2. Banding scale – between known specific bands within stratigraphic layers (e.g. shale band NS2 and the bands of BIF either side in the Newman Member).

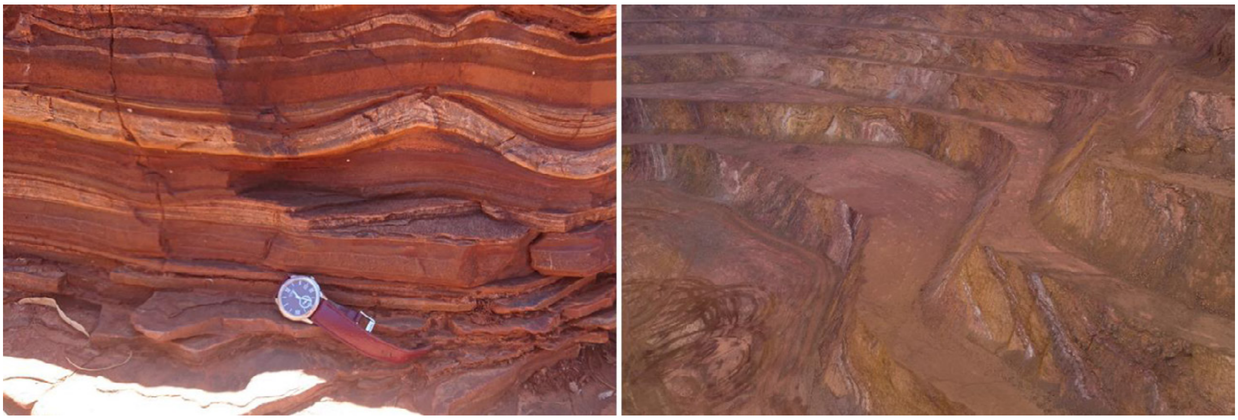

Figure 2: Scales of anisotropy in Western Australia iron ore deposits. Left: Bedding scale. Right: Banding scale in an iron ore pit with 12 metre high benches

Planar sliding along adversely oriented and low strength shale bands is the most common mode of slope instability from bench to overall slope scale in mining operations and also within natural slopes of the Pilbara region (Day & Seery, 2007; Eggers & Casparis, 2007; Bar, 2012; Joass et al. 2013; Lucas & de Graaf, 2013; Seery, 2015). The slope failure from the BHP mine discussed in this paper is a classic example of multi-bench planar sliding in the Hamersley Group (Figure 3). The failure itself was 'controlled' by means of a catchment bunds such that no personnel or equipment were exposed to the hazard, as shown in Figures 4 and 6 to 8.

Figure 3: Aerial reconnaissance of planar sliding failure mechanism at BHP mine

Rock mass and bedding shear strengths are typically well understood in the Pilbara region as relatively limited variation exists across individual deposits that are situated within the same stratigraphic unit (Bar & Weekes, 2017). Intact rock and rock mass shear strength, particularly in BIF-dominated stratigraphic units, may vary quite significantly with weathering, and to a lesser extent, alteration. No significant difference exists between the shear strength of bedding planes of shale and BIF units across the Pilbara (Maldonado & Haile, 2015; Maldonado & Mercer, 2019). The shear strength of shale bedding planes is also generally independent of weathering grade (Maldonado & Mercer, 2015). Failure back-analyses, site specific drilling & laboratory testing provide a means of assessing variation in shear strengths and material density. Slope stability analyses are undertaken considering the effects of anisotropy (Bar & Weekes, 2017):

- Bedding scale anisotropy can and should be modelled using directional shear strength models in 2D or 3D.
- Banding scale anisotropy is best modelled using discrete weak bands in both 2D and 3D models rather than with directional shear strength models.

The use of directional shear strength models for banding scale anisotropy allows the weakness plane to appear ubiquitously in this slope, rather than at its actual discrete location. This may result in over-conservatism. Seery (2015) conceptually compared using ubiquitous directional shear strength models against discretely located shale bands within the Dales Gorge Member of the Brockman Iron Formation. Seery (2015) concluded that the directional shear strength model did not necessarily honour the geology, particularly due to the widely spaced shale bands in the Dales Gorge Member. In order to achieve an optimal slope design, it is necessary to understand the geology, and have the ability to discretely model banding scale anisotropy (i.e. discretely model shale bands) coincidentally with bedding scale anisotropy. Notwithstanding this, it remains appropriate to use a ubiquitous shale band strength model however where the position of discrete shale bands is not known.

As slopes become exposed with mining progression, a detailed reconciliation process is used to validate the location of shale bands and enable a transition from a ubiquitous shale band strength model to discretely modelling banding scale anisotropy.

3 AERIAL RECONAISSANCE AND PHOTOGRAPHIC RECORDS

Aerial reconnaissance using UAV is routinely used to inspect unstable or failed slopes in both civil and mining engineering applications (Saroglou et al. 2019). High resolution imagery and video are captured while ensuring the geotechnical engineer or surveyor remains at a safe distance, away from the line-of-fire of potential rock falls or further instability. Figure 3 provides examples of aerial reconnaissance imagery from the planar sliding failure at the BHP iron ore mine. Failure geometry and geological conditions are illustrated in Figure 4, and ultimately comprised:

- Failure height of 24 metres.
- Failure width of 40 metres.
- Maximum horizontal runout of 5 metres on pit floor (contained within catchment bund), and
- Estimated failure size: 15,000 tonnes.

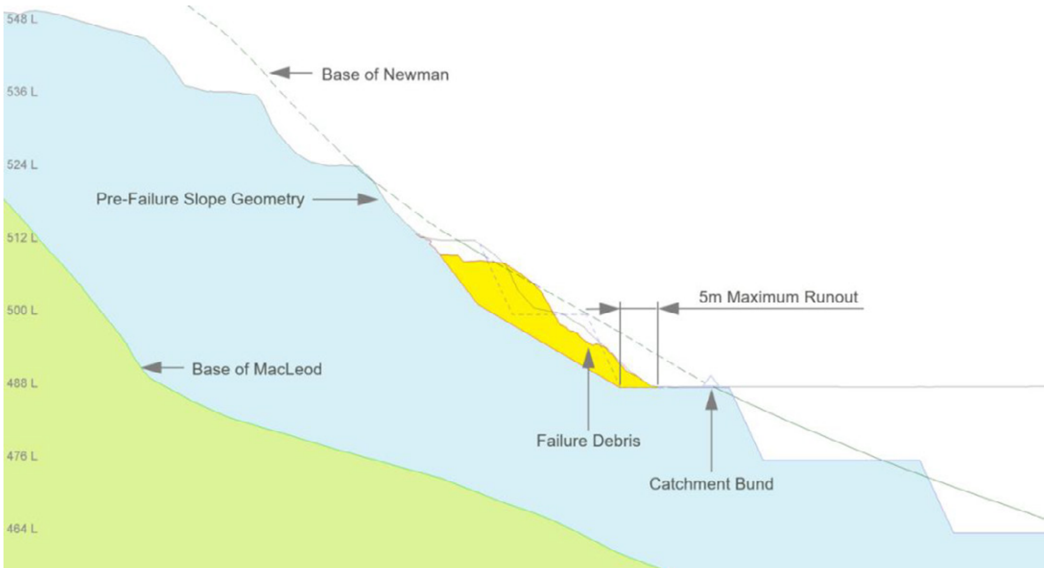

Figure 4: Geological Cross-Section through Failure

The planar failure mechanism was progressive, initiating as a local bench failure that propagated further with the progression of mining excavations and increased loading of the undercut shale band.

Figure 5 shows the pit slope prior to the failure with the pit floor on 500 RL in July 2019. Bedding planes near the convex slope profile are undercut and some shale bands exposed. Also visible are several areas of local bench crest losses.

Excavations progressed vertically downward 8 metres (pit floor 492 RL), undercutting a pervasive shale band and initiating a bench failure as shown in Figure 6.

Further excavation, vertically downward 4 metres (pit floor 488 RL) was successful in extracting ore and achieving the planned pit design; however, further deterioration of the initial bench failure was observed. Failure propagation was evident on 26 November 2019 as shown in Figure 7.

The rate of failure may have been exacerbated by 0.8 millimetres of rainfall that occurred on 27 November 2019, resulting in the 24 metre high failure shown in Figure 8.

Figure 5: Pit slope with undercut bedding planes near convex slope profile in July 2019 – pit floor 500 RL

Figure 6: Pit slope with initial 8 metre high failure contained within a rock fall catchment bund on 26 October 2019 – pit floor 492 RL

Figure 7: Pit slope failure propagation to 15 metre high contained within a larger failure catchment bund on 26 November 2019 – pit floor 488 RL

Figure 8: South Wall failure propagation to 24 m high on 27 November 2019 – pit floor 488 RL

4 UAV PHOTOGRAMMETRY AND GEOTECHNICAL MODEL UPDATE

Photogrammetry enables the generation of 3D models from a series of overlapping photographs. The introduction of the 'structure from motion' concept (Snavely, 2014) as well the broad availability of drones or UAV brought a renaissance of this technology. Structure from motion includes a series of processing steps that allows computing a comprehensive set of 3D surface points that are combined to a surface description (i.e. a mesh) in photo-realistic style. Due to the availability of redundant information, geometric deviations present in the camera used (i.e. lens distortion) are compensated for while generating the 3D model. This auto-calibration ability makes modern photogrammetry algorithms capable of producing accurate 3D models even from low-grade cameras, so even low cost, off-the-shelf drones can be used to generate 3D models at sufficiently high accuracy.

Several commercial software packages are available for modern photogrammetry (e.g. *Agisoft*, *Pix4D*, *ShapeMetriX*). All work in a similar way and provide comparable results. In this case study, *ShapeMetriX* software has been used since it also includes tools for geological and geotechnical mapping.

Figures 9 and 10 show the resultant 3D model generated from 284 photographs captured using a 9 millimetre digital camera mounted on a *DJI Phantom 4* drone. The model computed in less than one hour on a mobile workstation (*2017 Alienware 17 R4*). It consists of over 7 million surface points and has a ground sample distance (GSD) of 2 centimetres per pixel. Note the lighter, material on the right hand side of the model in Figure 10; this is where bench failures and crest losses had previously occurred on daylighting shale bands.

Model accuracy in that context needs to be looked at in at least two ways: (i) positional accuracy, i.e. the correct location of the 3D model and given coordinate grid or the correct orientation and scale of the model if working in local co-ordinates and (ii) shape accuracy that reflects mainly if all the details of the rough surface are rendered by the 3D model. It is linked with the GSD and spacing of the 3D surface points.

Positional accuracy is best if there are some reference points (ground control points or GCP) in the captured area. The GCPs are locations with surveyed coordinates. The referencing mechanism transforms the model to the location of the GCPs with remaining residuals in the sub-centimetre range.

In some cases, the installation and surveying of GCPs is time-consuming and costly especially in regions that are difficult to access such as alpine rock fall areas. Similarly, in an active mining area where personnel can be exposed to interaction with haul trucks and other mining equipment, GCPs may not be practicable from a safety perspective. In such case, the 3D model may be referenced (scaled and oriented) based only on GPS information recorded while taking the images. Such models show larger deviations from the ground truth - depending on the quality of GPS the absolute localisation might be some metres off. However, when comparing an accurately geo-localised 3D model using GCP and a roughly localised model using GPS, the scale and orientation of the 3D models align within 1% (i.e. shape accuracy is unaffected). Such pure GPS referencing can be even improved by using real time kinematic (RTK) or post processed kinematic (PPK). Both lead to better absolute geo-localisation of the 3D model without needing GCPs.

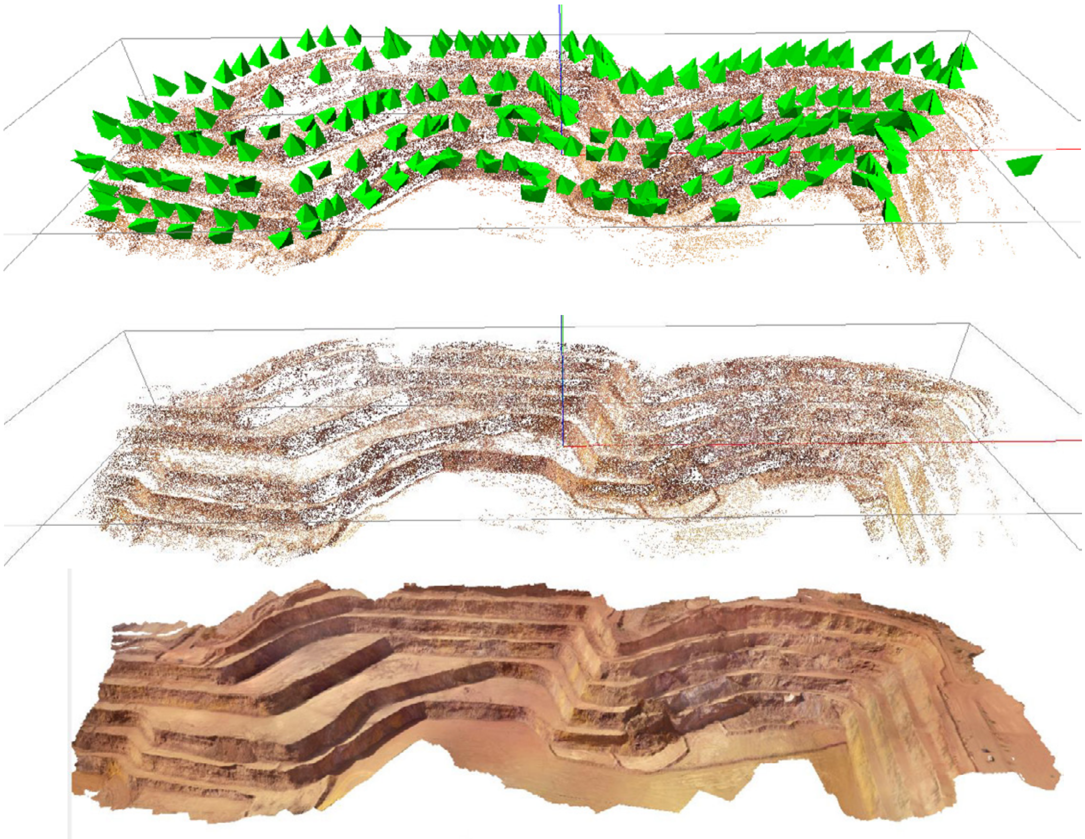

Figure 9: 3D model developed from UAV photogrammetry covering surface area of approximately 186,000m^2. Top: Location and orientation of photographs relative to point cloud; Middle: first pass 3D point cloud with >200,000 points; Bottom: detailed, dense 3D model comprising >7 million points and >2.6 million mesh elements

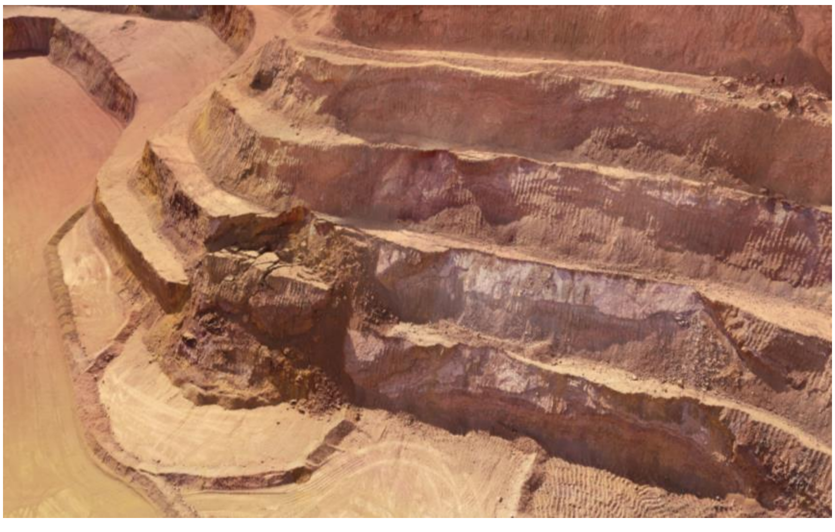

Figure 10: 3D model developed from UAV photogrammetry with the planar failure on the left hand side near the convex slope profile. Lighter coloured material on the right hand side where repeated bench crest losses have occurred shows near-planar shale bedding planes. Shape accuracy <5 centimetres without GCP

3D models developed from pure GPS referencing showed to be sufficiently scaled and oriented for performing geological mapping. In particular, data such as discontinuity orientations or spacing are practically unaffected since variations or errors in the 3D model (from UAV photogrammetry) are more than an order of magnitude less than errors obtained when using conventional measuring techniques such as mapping using a geological compass, tape measure or orienting and logging discontinuity orientations in drill core.

ShapeMetriX software allows direct analysis of geometric entities such as volumes, areas, distances, sections, and the measurement of point coordinates. In addition, geologically relevant features can be examined. By way of example, Figure 11 illustrates orientations of traces and surfaces that can be interpreted. Recent developments provide automatic analyses which leads to reproducible and statistically admissible assessments due to the high number of individual measurements (Buyer et al. 2018, Gaich et al. 2017, Kong et al. 2020, Riquelme 2014).

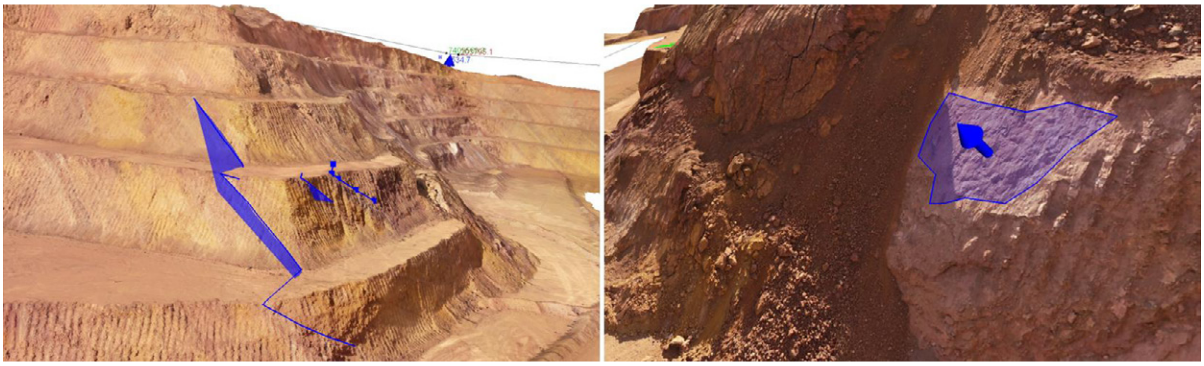

Figure 11: Left: Orientation measurement of significant shale bedding plane traces across multiple benches. Right: Shale bedding surface trace upon which planar sliding has already occurred

A total of 198 geological structures including bedding planes and joints were mapped using *ShapeMetriX* (Figure 12) and imported into a 3D CAD package (*GEM4D*) where the failure plane was modelled as a 3D surface. The failure plane was a distinct shale band that was located near the MacLeod – Newman geological contact. The orientation, or rather, the dip of this shale band was approximately 3-5° shallower than predicted in the pre-mining geological model, resulting in undercutting near the base of the slope (i.e. the pre-mining geological model was highly reliable).

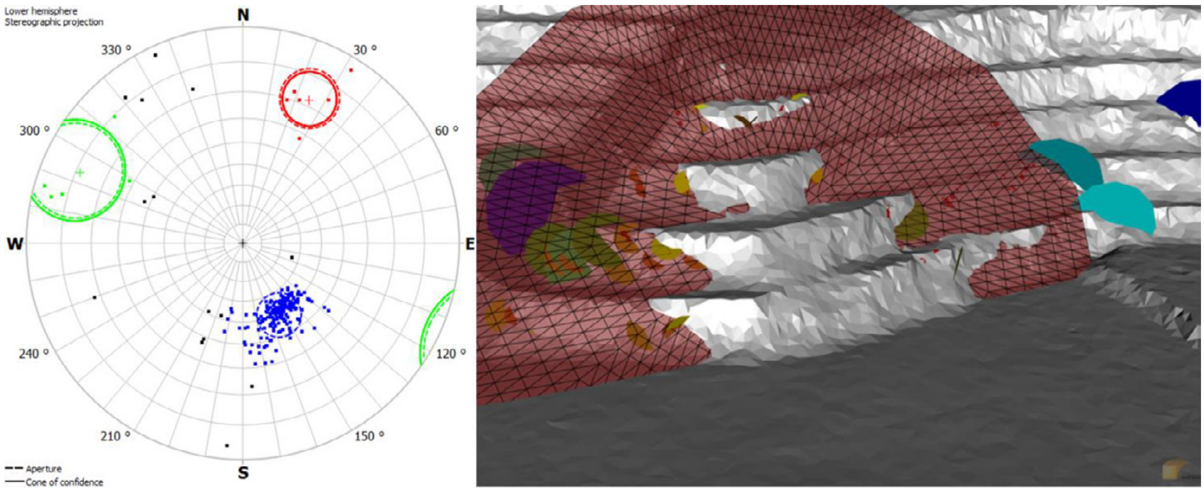

Figure 12: Left: stereographic projection showing bedding planes: 40°/333° (blue) and joints: 72°/205° (red) and 79°/113° (lime) in *ShapeMetriX*. Right: planar sliding failure plane (shale band) re-evaluated in *GEM4D* to create a wireframe mesh from utilizing the imported geological structures which are represented as coloured disks

5 SLOPE STABILITY ANALYSIS

5.1 2D AND 3D LIMIT EQUILIBRIUM MODELLING

Slope stability analyses can be undertaken in 2D or 3D. Traditionally, 2D models were generally most commonly constructed due to the relative ease of model construction and rapid computation time compared to 3D models (Wines, 2015).

2D models will generally yield a conservative result where: (i) the shear resistance of the end surfaces of failures is not included in the modelling process, and (ii) cross-sections selected for FoS (factor of safety) calculations are typically a worst-case scenario which will generally not be representative of all slope conditions (Duncan, 1996; Sjoberg, 1999; Wines, 2015). However, this is not always the case, where 3D analysis can also produce lower FoS than 2D analysis (Bromhead, 2004). Wines (2015) stated that the main reason for the differences in results between 2D and 3D analysis is the ability of 3D analysis to provide an accurate representation of the problem such as geometry, spatial distribution of geotechnical domains, discontinuity orientations and distribution of pore pressures, all of which are three-dimensional in reality.

Sjoberg (1999) and Wines (2015) stated that for relatively long open pits with basic geological conditions a 2D model can generally be justified, except at the pit corners and at the lateral bounds of slope failures. Lorig & Varona (2007) recommend 3D assessments of slope stability should be made where the strike of discontinuities is less than 20 to 30° from the strike of the excavated face. Bar & Weekes (2017) demonstrate that anisotropy (or true dip) of any structure can only be correctly modelled in 3D as 2D sections of a slope inherently result in an apparent dip which is not completely perpendicular to the anisotropy. Bar & McQuillan (2018) present several case studies from open pit iron ore and coal mines that highlight the limitation of 2D LE models in highly anisotropic geological settings. The case studies presented show 2D LE analysis can lead to either the over-estimation or under-estimation of FoS where 2D analysis did not adequately model the anisotropic conditions under which failure occurred.

McQuillan et al. (2019) states that to reliably predict the performance (e.g. propensity for failure) and critical failure mechanism (including spatial location) of slope failure, geotechnical engineers must select appropriate tools to complete slope stability assessments. Modelling techniques which can adequately account for the failure mechanisms typically observed in highly anisotropic geological settings, such as WAIO iron ore deposits, include empirical, 3D LE and 3D numerical (e.g. FE) modelling. Of these three methods, LE has become a preferred method for routine slope stability analysis since its introduction in the early 20th century. Its popularity stems from its ease of use, relatively fast calculation time and calibration from years of application and observation.

A FoS using LE methods can be calculated using the method of slices (2D analysis) or method of columns (3D analysis). Both methods are based on the principle of statics, where the summation of forces acting on a failure surface (i.e. mobilized stress) are compared with the sum of the forces available to resist failure (i.e. available shear resistance). The ratio between these two sums is defined as the FoS (Krahn, 2007). If the FoS is greater than 1, the slope is assumed to be stable. Geotechnical engineers frequently set design acceptance criteria (DAC) at values much higher than FoS = 1 when determining a stable slope design. That is, FoS of 1.2, 1.3, 1.5, etc. are required for varying slope configurations with varying required serviceability and strategic risk (Kirsten, 1983; Priest & Brown, 1983; Pothitos & Li, 2007; Gibson, 2011).

Rocscience Inc.'s Slide3 3D LE software has been used to calculate the FoS of the slope failure. The FoS calculated in Slide3 is based on the method presented by Cheng & Yip (2007). In Slide3 the sliding mass, in the form of part of a sphere, ellipsoid or complex surface, is discretised into vertical columns as shown in Figure 13 (Cheng & Yip, 2007). Forces are analogous to the vertical slice method used in 2D. In 3D, each column has a share cross-section and forces and moments are solved in two orthogonal directions. Vertical forces determine the normal and shear force acting on the base of each column (Cheng & Yip 2007, McQuillan et al. 2018).

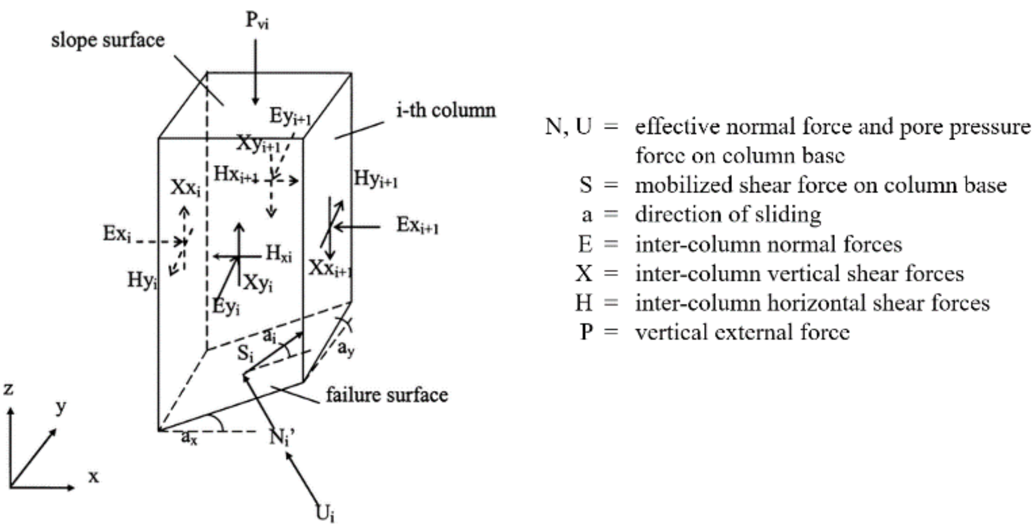

Figure 13: Forces acting on an individual 3D column as per Slide3 LE method of columns (Cheng & Yip, 2007)

5.2 PRE-MINING GEOTECHNICAL DESIGN

The pit slopes predominantly include the Nammuldi and MacLeod members of the Marra Mamba Iron Formation as illustrated in Figure 14. Mineralisation is hosted within the Newman member, which also appears locally within the slope in areas where both slope and stratigraphical geometries permit, including the region of failure. The current pit is significantly above the groundwater table, so dry conditions are appropriate for the slopes.

Table 1 presents the original geotechnical design shear strength parameters derived from diamond core drilling and laboratory testing using:

- Hoek-Brown failure criterion for rock mass (Hoek & Brown, 1980; Hoek et al. 2002).
- Mohr-Coulomb and Patton failure criteria for bedding (Patton, 1966). Note: the Barton-Bandis failure criterion is also commonly applied where available data permits (Barton, 1976; Barton & Bandis 1990).

Directional shear strength models were applied to all 2D LE analyses as described by Bar & Weekes (2017) to apply reduced shear strength in the orientation of both BIF and shale bedding planes with respect to the surrounding rock mass.

2D LE analysis was used to design the pit slopes to meet the DAC whereby the FoS was equal to, or greater than, 1.2 for inter-ramp and overall slopes. The original (pre-mining) geotechnical design for the pit identified single to multiple bench scale hazards on the south wall using a combination of 2D LE and kinematic analyses from which the probability of undercutting bedding planes was expected to be in the order of 50%. As such, the area was routinely inspected and included as part of the slope validation process whereby actual ground conditions are reconciled against original geotechnical design predictions (Dixon et al. 2011).

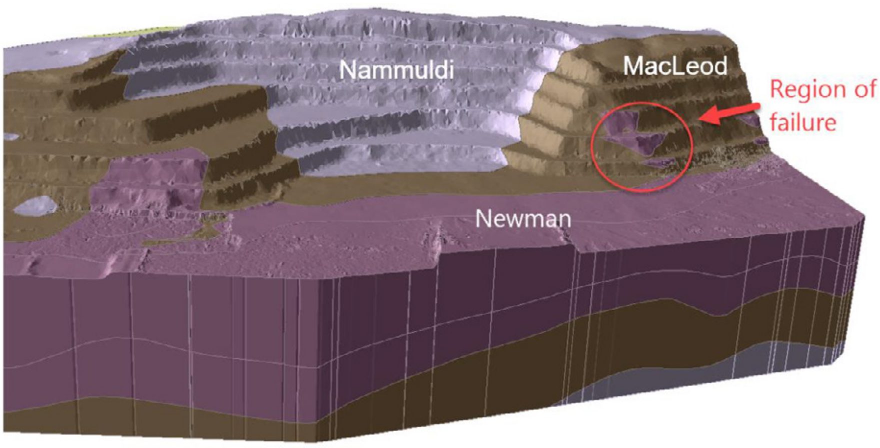

Figure 14: Updated geotechnical model for south wall represented in 3D for LE analysis using *Slide3*

Table 1: Geotechnical Model – Initial Shear Strength Parameters

Geotechnical Domain	Unit Weight (kN/m³)	Rock Mass			Anisotropy (Bedding)		Waviness (°)
		UCS (MPa)	GSI	m_i	c' (kPa)	ϕ' (°)	
Newman	31	15	33	10	0*	29	0
MacLeod	28	37	37	8	0*	29	12
Nammuldi	25	15	34	8	0*	29	0
Jeerinah	21	15	21	6	0*	29	0

** Zero cohesion & linear shear strength behaviour are in some instances, conservative inputs where limited site specific data was available during the original geotechnical design.*

During the course of mining five benches (i.e. vertically downward 60 metres), several local single bench failures ≤ 12 metres in height had occurred, either during blasting, or excavation. These were safely remediated with standard mining procedures. Using the 3D model developed from UAV photogrammetry, Figure 15 reconciles the actual percentage of slope face area that had been involved with failure events. The failure areas represent 32% of the total slope area (i.e. slope performance was better than expected since this is significantly less than the predicted 50% from probability of undercutting assessments).

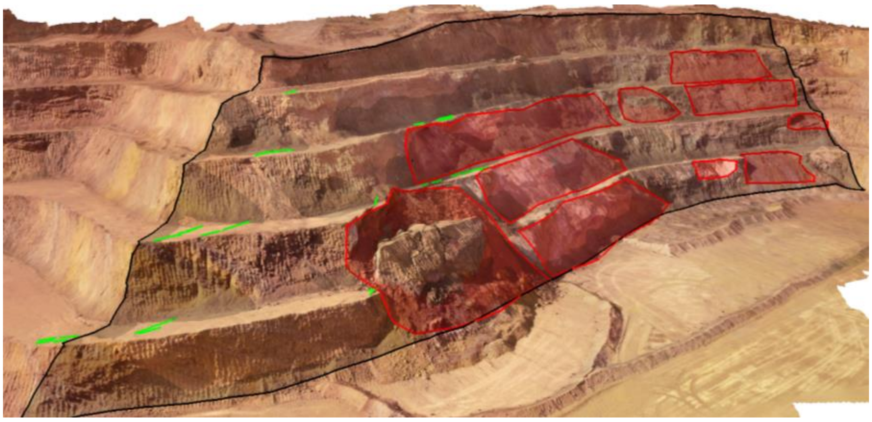

Figure 15: UAV Photogrammetry 3D model illustrating failure event areas in red; total failure area in black; and visible tension crack traces in lime green using *ShapeMetriX*

5.3 3D LIMIT EQUILIBRIUM BACK-ANALYSIS OF FAILURE

The 24 metre high planar failure in Figure 3 was back-analysed to refine the original geotechnical design shear strength parameters to enable added rigour to the geotechnical model and enable better prediction of future ground behaviour as mining continues. The 3D LE model was developed such that it is spatially large enough to enable subsequent re-evaluation of future pit slope stability and alternative designs, if required.

The updated geotechnical model including the location and orientation of the failure plane (shale bedding) and updated stratigraphic wireframes derived from UAV photogrammetry were utilized in the 3D LE back-analysis.

Back-analysis focused on shale bedding in the vicinity of the MacLeod-Newman geological contact at low confining stress with overburden ranging from 5 to 12 metres. Anisotropy (bedding) shear strength parameters were adjusted to obtain a FoS = 1 ± 0.01 while attaining realistic slip surfaces representative of the actual planar sliding failure (Table 2).

Table 2: Planar Sliding Failure Back-Analysis in 3D LE using *Slide3*

Geotechnical Domain	Anisotropy (Bedding)		FoS	FoS Method of Columns	Failure Volume (m^3)	Reference
	c' (kPa)	ϕ' (°)				
MacLeod – Newman Contact: Shale	0	29	1.002 – 1.026	Janbu – GLE	1060	Figure 16
	0	28	0.965 – 1.017	Janbu – GLE	1070	-
	5	26	1.009 – 1.077	Janbu - GLE	5900	Figure 17

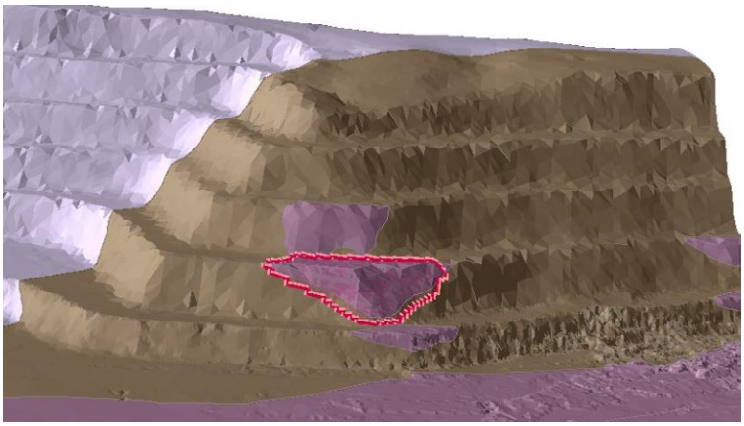

Figure 16: Planar sliding failure back-analysis using bedding shear strength parameters, c’=0 kPa and ϕ’=29°, identifying initial single bench instability

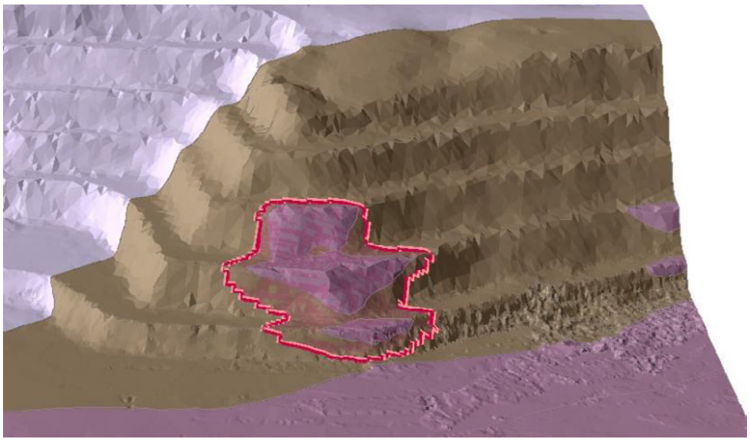

Figure 17: Planar sliding failure back-analysis using bedding shear strength parameters, c'=5 kPa and ϕ'=26˚, identifying larger mechanism

The 3D LE back-analyses results indicated bedding shear strengths likely contained 0 to 5 kPa of cohesion with friction angles ranging from 26 to 29 degrees.

Vibration and gas pressures from blasting along the already weaker shale bedding planes likely resulted in a loss, or at least significant degradation, of cohesion, that initiated the planar failure.

5.4 RE-EVALUATION OF FUTURE PIT SLOPE DESIGN

The future pit slope design was re-evaluated based on the bedding shear strengths obtained from the back-analysis as well as updated stratigraphical wireframes derived from the UAV photogrammetry. Figure 18 illustrates key findings of the 3D LE analysis results of the future pit slope:

- FoS=1.09 for a single bench failure mechanism was identified. Although not complying with the design acceptance criteria, associated risks of a potential failure can be managed through the wide catchment berm as well as slope deformation monitoring.
- FoS=1.20 for a 48 metre high multiple bench slope was identified and complied with the DAC. Notwithstanding this, slope validation will routinely continue with mine progression to ensure that if any significant deviations to the geotechnical model are observed, they can be acted upon.
- No evidence of larger slope failure risks using the updated geotechnical model.

Figure 18: 3D LE models evaluating stability of future pit slope design using bedding shear strength parameters, c'=5 kPa and ϕ'=26˚. Left: FoS=1.09 for single 12 metre high bench; Right: FoS=1.2 for 48 metre high multiple bench slope

6 DISCUSSION

Aerial reconnaissance, photogrammetry and 3D LE modelling were used to rapidly appraise ground conditions and stability conditions for the current and future planned slopes at Jimbebar iron ore mine. Table 3 demonstrates that through the use of the latest tools and technology, the process can be successfully completed in less than 12 hours. The ability to respond quickly to geotechnical events enables the geotechnical team to provide quality advice to mine operation to continue operating safely and economically.

The ease and speed of undertaking UAV photogrammetry makes it a powerful tool for identifying the location, orientation and length of geological structures. However, it should be noted that photogrammetry application on its own remains limited in its capability of undertaking complete ground characterization. By way of example, joint properties such as infilling and intact rock parameters such as strength cannot be evaluated or estimated using this method and required physical time spent in the field where safely accessible.

The BHP WAIO survey team uses UAV photogrammetry for routine end-of-month surveying. With the addition of minor extra flights to capture additional angles and higher resolution digital SLR camera photographs, the geotechnical engineering and geology teams are also enabled to routinely update geotechnical and structural geological models across operating pits. Future improvements to the process include the use of high-precision UAV that remove the need for ground control points while maintaining or improving aerial reconnaissance and photogrammetry accuracy.

Table 3: Slope Failure Appraisal Tasks and Timing

Task	Personnel	Time Taken (hours)	Tools Required / Used
Aerial Reconnaissance and Photogrammetry Field Work	Survey and Geotechnical Engineering	2	*DJI Phantom 4* UAV
Photogrammetry Processing and 3D Model Generation	Geotechnical Engineering	< 1	*Shapemetrix UAV* software
Mapping Geological Features	Geotechnical Engineering	1	*Shapemetrix UAV* software
Updating Geotechnical Model including Local Stratigraphic Wireframes	Geotechnical Engineering	2	*GEM4D* and *Vulcan* software
3D LE Modelling: Failure Back-Analysis	Geotechnical Engineering	3	*Slide3* software
3D LE Modelling: Future Pit Slope Design	Geotechnical Engineering	1	*Slide3* software

7 CONCLUSION

Since mid-2019, the WAIO geotechnical engineering team has routinely been analysing pit slope stability using 3D LE software *Slide3*. The shift to 3D modelling from 2D cross-sections has facilitated better integration with mine planning and is increasing the speed (and quality) at which we can review proposed pit slope designs. Quite simply, new mine and pit slope designs are inserted into a 3D model, replacing their predecessor. This approach also has the ability to automatically generate and analyse 2D cross-sections that are directly comparable with historic analyses. The 3D models themselves provide significant insight into possible lateral extents of failure mechanisms such that sensible advice can be provided to mine operations in terms of geotechnical risk management without the need for overly conservative slope designs.

8 ACKNOWLEDGEMENTS

The authors would like to acknowledge the efforts of Blair Chalmers, Shaun van Goor and Michael Marchetti of the BHP WAIO Survey team for their prompt response and efforts with aerial reconnaissance as well as their enthusiasm for integrating new technologies into procedures to add value and save time and costs. The authors would also like to acknowledge the support of Calvin Snodgrass and Annabelle Blom, *past and present* Head's of Resource Engineering, for supporting technology and system improvements across the technical disciplines at BHP WAIO.

9 REFERENCES

Bar, N. (2012). Performance driven slope management, design and optimization at Brockman Operation, Rio Tinto Iron Ore. *Proc. 9th Young Geotechnical Professionals Conference (9YPGC)*, Melbourne, Australia, 19-24.

Bar, N. and Barton, N. (2017). The Q-Slope Method for Rock Slope Engineering. *Rock Mechanics and Rock Engineering*, 50(12), 3307-3322.

Bar, N. and Barton, N. (2018). Q-Slope: An Empirical Rock Slope Engineering Approach in Australia. *Australian Geomechanics Journal*, 53(4), 73-86.

Bar, N. and McQuillan, A. (2018). 3D Limit Equilibrium Slope Stability Analysis for Anisotropic and Faulted Rock Masses in Australian Coal and Iron Ore Mines, *Proc. ISRM International Symposium - ARMS10*, Singapore, 12p.

Bar, N. and Weekes, G. (2017). Directional shear strength models in 2D and 3D limit equilibrium analyses to assess the stability of anisotropic rock slopes in the Pilbara region of Western Australia. *Australian Geomechanics Journal*, 52(4), 91-104.

Bar, N., Weekes, G. and Welideniya S. (2018). Benefits and limitations of applying directional shear strengths in 2D and 3D limit equilibrium models to predict slope stability in highly anisotropic rock masses. *Proc. Eurock 2018: Geomechanics and Geodynamics of Rock Masses*, Saint Petersburg, Russian Federation, 6p.

Bar, N., Yacoub, T.E. and McQuillan, A. (2019). Analysis of a large open pit mine in Western Australia using finite element and limit equilibrium methods. *Proc. ARMA 2019: 53rd US Rock Mechanics / Geomechanics Symposium*, New York, United States of America.

Barton, N. (1976). The shear strength of rock and rock joints. *Int. J. Min. Sci. & Geomech. Abstr.* 13(10), 1-24.

Barton, N. and Bandis, S. (1990). Review of predictive capabilities of JRC-JCS model in engineering practice. *In Rock joints, Proc. Int. Symp. on Rock Joints*, Loen, Norway, 603-610.

Barton, N. and Bar, N. (2015). Introducing the Q-slope method and its intended use within civil and mining engineering projects. *Future Development of Rock Mechanics; Proc. ISRM Reg. Symp. Eurock 2015 & 64th Geomechanics Colloquium*, Salzburg, Austria, 157-162.

Barton, N. and Quadros, E. (2015). Anisotropy is Everywhere, to See, to Measure, and to Model, *Rock Mechanics and Rock Engineering*, 48(4), 1323-1339.

Bromhead, E. (2004). Landslide slip surfaces: their origins, behavior and geometry, *Landslides: Evaluation and Stabilization*, Taylor & Francis Group, London.

Buyer, A., Pischinger, G. and Schubert, W. (2018). Image-based discontinuity identification. *Geomechanics and Tunnelling*, 11(6), 693-700.

Cheng, Y. and Yip, C. (2007). Three-dimensional asymmetrical slope stability analysis extension of Bishop's, Janbu's, and Morgenstern-Price's techniques. *J. Geotech. Geoenviron. Eng*, 133(12), 1544-1555.

Dalstra, H.J. (2014). Structural evolution of the Mount Wall region in the Hamersley Province, Western Australia and its control on hydrothermal alteration and formation of high-grade iron deposits. *Journal of Structural Geology*, 67, 268-292.

Day, A.P. and Seery, J.M. (2007). Monitoring of a Large Wall Failure at Tom Price Iron Ore Mine. *Proc. Int. Symp. on Rock Slope Stability in Open Pit Mining and Civil Engineering – Slope Stability 2007*, Perth, Australia, 333-340.

Dixon, R.A., Johnson, T.M., de Graaf, P.J.H., Wessels, S.D.N. and Venter, J. (2011). Risk Based Geotechnical Slope Reconciliation at Rio Tinto Iron Ore, Pilbara Operations. *Proc. Int. Symp. on Rock Slope Stability in Open Pit Mining and Civil Engineering – Slope Stability 2011*, Vancouver, Canada, 14p.

Duncan, J. (1996). State of the art: Limit equilibrium and finite-element analysis of slopes. *J. Geotech. Engng*, 122(7), 577-596.

Eggers, M.J. and Casparis, D.L. (2007). Pit Slope Design in Pilbara Iron Deposits - Deposit A West Angelas, Western Australia. *Proc. Int. Symp. on Rock Slope Stability in Open Pit Mining and Civil Engineering – Slope Stability 2007*, Perth, Australia, 463-476.

Gaich, A., Pötsch, M. and Schubert, W. (2017). Digital rock mass characterization 2017. Where are we now? – What comes next? *Geomechanics and Tunnelling*, 10(5), 561-567.

Gibson, W. (2011). Probabilistic methods for slope analysis and design. *Australian Geomechanics Journal*. 46(3), 29-39.

Harmsworth, R.A., Kneeshaw, M., Morris, R.C., Robinson, C.J. and Shrivastava, P.K. (1990). BIF-derived iron ores of the Hamersley Province. *Geology of the Mineral Deposits of Australia and Papua New Guinea (Australasian Institute of Mining and Metallurgy Monograph 14),* 1, 617-642.

Hoek, E. and Brown, E.T. (1980). Empirical strength criterion for rock masses. *J. Geotech. Engng Div.*, *ASCE*, 106 (GT9), 1013-1035.

Hoek, E., Carranza-Torres, C.T. and Corkum, B. (2002). Hoek-Brown failure criterion – 2002 edition. *Proc. 5th North American Rock Mechanics Symposium*, Toronto, Canada, 267-273.

Joass, G.G., Dixon, R., Sikma, T., Wessels, S.D.N., Lapwood, J. and de Graaf, P.J.H. (2013). Risk Management and Remediation of the North Wall Slip, West Angelas Mine, Western Australia. *Proc. International Symposium on Rock Slope Stability in Open Pit Mining and Civil Engineering – Slope Stability 2013*, Brisbane, Australia, 1-16.

Kirsten, H. (1983). Significance of the probability of failure in slope engineering. *The Civil Engineer in South Africa*, 25(1), 17-27.

Kong, D., Wu, F. and Saroglou, C. (2020). Automatic identification and characterization of discontinuities in rock masses from 3D point clouds. *Engineering Geology*, 265(105442), 16p.

Krahn, J. (2007). Limited equilibrium, strength summation and strength reduction methods for assessing slope stability. *Proc. 1st Canada-US Rock Mechanics Symposium*, Vancouver, Canada, 311-318.

Lorig, L. and Varona, P. (2007). Numerical Analysis, *Rock Slope Engineering, Civil and Mining,* 4th Edition. C. Wyllie and C.W. Mah (eds). Spon Press.

Lucas, D.L. and de Graaf, P.J.H. (2013). Iterative geotechnical pit slope design in a structurally complex setting: a case study from Tom Price, Western Australia. *Proc. International Symposium on Rock Slope Stability in Open Pit Mining and Civil Engineering – Slope Stability 2013*, Brisbane, Australia, 513-526.

Maldonado, A. and Haile, A. (2015). Application of ANOVA and Tuckey-Cramer statistical analysis to determine similarity of rock mass strength properties across Banded Iron Formations of the Pilbara region in Western Australia. *Proc. SAIMM Slope Stability 2015*, Cape Town, South Africa, 15-33.

Maldonado, A. and Mercer, K.G. (2015). An investigation into the shear strength of bedding planes in shale materials from the Hamersley Group rocks in the Pilbara region of Western Australia. *Proc. SAIMM Slope Stability 2015*, Cape Town, South Africa, 47-62.

Maldonado, A. and Mercer, K.G. (2018). Comparison of the laboratory and Barton-Bandis derived shear strength of bedding partings in fresh shales of the Pilbara, Western Australia. *Proc. ISRM International Symposium - ARMS10*, Singapore, 13p.

McQuillan, A. (2019). A risk-based slope stability assessment methodology (SSAM) for excavated coal mine slopes. *PhD Thesis*, University of New South Wales, Australia, 318p.

McQuillan, A., Canbulat, I. and Oh, J. (2019). Methods applied in Australian industry to evaluate coal mine slope stability. *International Journal of Mining Sciences and Technology*, 5p.

McQuillan, A., Canbulat, I., Payne, D. and Oh, J. (2018). New risk assessment methodology for coal mine excavated slopes. *International Journal of Mining Sciences and Technology*, 28(4), 583-592.

Pastor, J.L., Riquelme, A.J., Tomás, R. and Cano, M. (2019). Clarification of the slope mass rating parameters assisted by SMRTool, an open-source software. *Bulletin of Engineering Geology and the Environment*, 78(8), 6131-6142.

Patton, F.D. (1966). Multiple modes of shear failure in rock. *Proc 1st ISRM Congress*, Lisbon, Portugal, 509-513.

Perring, C. and Hronsky, J. (2019). Guide to the Geology of the Hamersley Iron Ore Province: The Blue Book II, *BHP Limited Internal Document*, 134p.

Pothitos, F. and Li, T. (2007). Slope design criteria for large open pits: case study. *Proc. Int. Symp. on Rock Slope Stability in Open Pit Mining and Civil Engineering – Slope Stability 2007*, Perth, Australia, 341-352.

Priest, S. and Brown, E. (1983). Probabilistic stability analysis of variable rock slopes. *Institution of Mining and Metallurgy Transactions*, 92, A1-A12.

Riquelme, A.J., Abellán, A., Tomás, R. and Jaboyedoff, M. (2014). A new approach for semi-automatic rock mass joints recognition from 3D point clouds. *Computers & Geosciences*, 68, 38-52.

Romana, M. (1985). New adjustment ratings for application of Bieniawski classification to slopes. *Proc. ISRM Int. Symp. Rock Mechanics in Excavations for Mining and Civil Works*, Zacatecas, Mexico, 49-53.

Romana, M. (1995). The geomechanical classification SMR for slope correction. *Proc. 8th ISRM Congress on Rock Mechanics*, Tokyo, Japan, 1085-1092.

Saroglou, C., Kallimogiannis, V., Bar, N., Manousakis, G. and Zekkos, D. (2019). Analysis of slope instabilities in the Corinth Canal using UAV-enabled mapping. *Proc. ICONHIC 2019*, Chania, Greece, 8p.

Seery, J.M. (2015). Limit equilibrium analysis of a planar sliding example in the Pilbara Region of Western Australia – comparison of modelling discrete structure to three anisotropic shear strength models. *Proc. SAIMM Slope Stability 2015*, Cape Town, South Africa, 681-696.

Sjoberg, J. (1999). Analysis of Large Scale Rock Slopes, *PhD Thesis*, Lulea University of Technology Department of Civil and Mining Engineering Division of Rock Mechanics, Sweden.

Snavely, N., Seitz, S.M. and Szeliski, R. (2008). Modeling the World from Internet Photo Collections. *International Journal of Computer Vision*, 80(2), 189-210.

Wines, D. (2015). A comparison of slope stability analyses in two and three dimensions. *Proc. SAIMM Slope Stability 2015*, Cape Town, South Africa, 305-316.